Author Manuscript

Author Manuscript

Author Manuscript

Author Manuscript

HHS Public Access

Author manuscript

Auton Neurosci. Author manuscript; available in PMC 2024 July 01.

Published in final edited form as:

Auton Neurosci. 2023 July ; 247: 103095. doi:10.1016/j.autneu.2023.103095.

Hypoxia Augments TRPM3-mediated Calcium Influx in Vagal Sensory Neurons

Katherine R. Langen,

Heather A. Dantzler,

Procopio Gama de Barcellos-Filho,

David D. Kline

Dept. of Biomedical Sciences, Medical Pharmacology and Physiology, and Dalton Cardiovascular Research Center, University of Missouri 134 Research Park Drive, Columbia, Missouri 65211

Abstract

Transient receptor potential melastatin 3 (TRPM3) channels contribute to nodose afferent and brainstem nucleus tractus solitarii (nTS) activity. Exposure to short, sustained hypoxia (SH) and chronic intermittent hypoxia (CIH) enhances nTS activity, although the mechanisms are unknown. We hypothesized TRPM3 may contribute to increased neuronal activity in nTS-projecting nodose ganglia viscerosensory neurons, and its influence is elevated following hypoxia. Rats were exposed to either room air (normoxia), 24-hr of 10% O_2 (SH), or CIH (episodic 6% O_2 for 10d). A subset of neurons from normoxic rats were exposed to *in vitro* incubation for 24-hr in 21% or 1% O_2. Intracellular Ca^{2+} of dissociated neurons was monitored via Fura-2 imaging. Ca^{2+} levels increased upon TRPM3 activation via Pregnenolone sulfate (Preg) or CIM0216. Preg responses were eliminated by the TRPM3 antagonist ononetin, confirming agonist specificity. Removal of extracellular Ca^{2+} also eliminated Preg response, further suggesting Ca^{2+} influx via membrane-bound channels. In neurons isolated from SH-exposed rats, the TRPM3 elevation of Ca^{2+} was greater than in normoxic-exposed rats. The SH increase was reversed following a subsequent normoxic exposure. RNAScope demonstrated TRPM3 mRNA was greater after SH than in Norm ganglia. Incubating dissociated cultures from normoxic rats in 1% O_2 (24-hr) did not alter the Preg Ca^{2+} responses compared to their normoxic controls. In contrast to in vivo SH, 10d CIH did not alter TRPM3 elevation of Ca^{2+}. Altogether, these results demonstrate a hypoxia-specific increase in TRPM3-mediated calcium influx.

Keywords

afferent signaling; baroreflex; calcium; hypoxia; ion channels; TRPM3

Corresponding Author: David D. Kline, Ph.D., Dalton Cardiovascular Research Center, Dept of Biomedical Sciences, University of Missouri, 1500 Research Park Dr., Columbia, MO 65211, USA, klinedd@missouri.edu, +1 573 884-0505.

Author contributions: D.D.K. designed the study. KRL, HAD and PBdG performed and analyzed the data. All interpreted the data. KRL and DDK wrote the manuscript and prepared figures. All approved final version.

Conflict of Interest: The authors declare no competing financial interests.

Publisher's Disclaimer: This is a PDF file of an unedited manuscript that has been accepted for publication. As a service to our customers we are providing this early version of the manuscript. The manuscript will undergo copyediting, typesetting, and review of the resulting proof before it is published in its final form. Please note that during the production process errors may be discovered which could affect the content, and all legal disclaimers that apply to the journal pertain.

Author Manuscript Author Manuscript Author Manuscript Author Manuscript

1. INTRODUCTION

Vagal afferents are critical to a variety of homeostatic functions including the regulation of heart rate and blood pressure via the arterial baroreflex. Aortic baroreceptors have their viscerosensory afferent somas within the nodose ganglia where their central projections terminate and are integrated within the brainstem nucleus tractus solitarii (nTS, (Kupari et al., 2019; Min et al., 2019)). The ionic mechanisms by which these sensory afferents maintain resting activity and overall cardiovascular homeostasis, as well as afferent elevation in activity upon a stressor, is not completely understood (Schild et al., 2012). Recent studies have suggested a role of transient receptor potential (TRP) channels in these activities. TRP channels are expressed within sensory neurons and the nTS and channel activation elevate sensory activity and the release of glutamate from their centrally projecting processes (Kline et al., 2019; Ragozzino et al., 2021). Within the nodose ganglia, TRPV1, TRPA1, TRPM3 and TRPM8 are expressed or functionally relevant (Hondoh et al., 2010; Jawaid et al., 2022; Kline et al., 2019; Ragozzino et al., 2021). Recently TRPM3, a member of the melastatin subfamily of TRP channels, has been shown to increase intracellular calcium and depolarize nodose sensory neurons, co-express with TRPV1, and elevate glutamate release in the nTS (Ragozzino et al., 2021).

Exposure to hypoxia (low oxygen) is a systemic stressor observed in a variety of diseases as well as high altitude ascent. Hypoxia is sensed by the peripheral carotid body chemoreceptors whose adjacent chemosensory somas lie in the petrosal ganglion and project to the nTS (Prabhakar et al., 2002). Upon exposure to hypoxia, respiration and sympathetic activity is elevated, with the latter offsetting the hypoxia-induced vasodilation. Hypoxia also augments glutamatergic signaling integration in the nTS (Kline et al., 2007; Matott et al., 2020). Several lines of evidence suggest TRP channels may contribute to the physiological response to hypoxia. For instance, the carotid body and chemoafferent soma containing petrosal ganglia express TRPM3 (Shirahata et al., 2015). Nonspecific block of TRP channels, including TRPM3, attenuates the chemosensory nerve response to hypoxia (Shirahata et al., 2015). Chronic intermittent hypoxia (CIH), a rodent model of the hypoxia induced by obstructive sleep apnea, increases TRPV1 protein and afferent-released glutamate (Kline et al., 2019). In addition, TRPA1 is activated by hypoxia and increases vagal neuronal discharge (Mori et al., 2017), where TRPA1 knockout attenuates arousal to mild hypoxia (Chen et al., 2020). Given the expression of TRP channels in the vagal afferent arc and their contribution to neuronal activity to hypoxic stimuli, this study investigated the possible contribution of TRPM3 in afferent activity following two unique hypoxia exposures, short, 1-day sustained hypoxia and 10-day CIH. We show that TRPM3 activation elevates intracellular calcium, and this elevation is exaggerated only after sustained hypoxia.

2. MATERIAL and METHODS

2.1 Animals.

All experiments were conducted following the National Institutes of Health Guide for the Care and Use of Laboratory Animals guidelines and protocols were approved by the University of Missouri Animal Care and Use Committee. Male Sprague-Dawley rats

Author Manuscript Author Manuscript Author Manuscript Author Manuscript

between 3 and 6 weeks were used for all experiments. They were housed in standard rat cages up until experimentation in a 12:12 hour light-dark cycle room held at 22°C and 40% humidity and were given ad libitum access to food and water.

2.2 Neuronal experimental groups.

The influence of TRPM3 on Ca^{2+} influx was tested on nodose neurons after one of the following experimental conditions. *Control* cells consisted of isolated neurons from naïve rats. *In vitro* hypoxia exposure included neurons that were initially dissociated from naive rats. The influence of TRPM3 on Ca^{2+} influence was studied in this group to eliminate the potential influence of neuronal and/or humoral activity that may occur during in vivo hypoxia. For each culture half the plates were incubated for 24-hr in a 21% O_2, 5% CO_2 atmosphere (*24-hr in vitro normoxia)*, whereas the other half were exposed for 24-hr in 1% O_2, 5% CO_2 (*24-hr in vitro hypoxia)*. In vivo hypoxia exposure cells consisted of neurons dissociated from rats exposed to 24hr of SH (10% O_2) or 10d of CIH as detailed below. A comparable normoxic exposure (24 hr or 10d) were used as in vivo controls. To examine the potential reversibility of SH exposure, cells were isolated from rats exposed to 10% O_2 for 24-hr followed by 21% O_2 for 24-hr (*48-hr hypoxia-normoxia)*. Control cells consisted of neurons isolated from rats exposed to 21% O_2 for 48-hr (*48-hr normoxia).*

2.3 In vitro and in vivo sustained and chronic intermittent hypoxic exposure.

In vitro hypoxic exposure occurred in neurons dissociated from naïve rats. Following cell isolation and plating, petri dishes containing nodose neurons were placed in a humidified hypoxic incubator chamber (Stem Cell Technologies) flushed with either 21% O_2, 5% CO_2 (normoxia) or 1% O_2, 5% CO_2 (hypoxia). The hypoxic incubator chamber was then placed in a standard incubator (37° C, 21% O_2, 5% CO_2) for 24-hr.

In vivo hypoxic exposure consisted of placing unrestrained naïve rats housed in standard rat cages within a commercially available hypoxic system (BioSpherix, Redfield, NY). Sustained hypoxia (SH) consisted of reducing environmental oxygen to 10% O_2 via infusion of nitrogen. SH exposure was 24 hrs for 1 day (Matott et al., 2020). CIH exposure consisted of alternating cycles of 21% and 6% oxygen (~ 45s), 10 episodes/hr, 8 hr/day between 9am-5pm; during the animals' normal inactive period. Between 5pm and 9am animals were maintained at room air (Kline et al., 2009; Kline et al., 2007; Kline et al., 2019). Inspired oxygen levels were maintained via a feedback system and addition of pure oxygen or nitrogen. Normoxic animals consisted of rats housed in standard rat cages placed in the hypoxic chamber but only exposed to 21% O_2. Ambient oxygen, carbon dioxide, temperature, and humidity levels were continuously monitored.

2.4 Visceral neuron dissociation and culture.

Following normoxic or hypoxic exposure, rats were anesthetized with isoflurane and decapitated. As previously (Dantzler et al., 2020; Kline et al., 2009), the left and right nodose ganglia were isolated, removed, placed in ice cold DMEM-F12 (Dulbecco's Modified Eagle Medium/Nutrient Mixture F-12; Gibco cat# 11320-033) and minced with microdissection scissors. The tissue was then removed from DMEM-F12 and placed in a 10 mL Hanks Balanced Salt Solution (Gibco cat# 14175-095) containing Collagenase

Author Manuscript Author Manuscript Author Manuscript Author Manuscript

Type 2 (335 U/mL; Worthington Biochemical Corporation cat# LS004176) and Dispase (Neutral Protease AOF; 0.5 U/mL; Worthington Biochemical Corporation cat# LS02109) and left in a shaking water bath for 3 intervals of 15 minutes, with a gentle trituration with a glass pipette between the intervals. A final, thorough trituration then occurred in 10 mL of DMEM-F12-based growth media containing DNase with $MgCl_2$ (Thermo Scientific cat# EN0521), and Bovine Serum Albumin (BSA; Sigma-Aldrich cat# A4378). The cell suspension was filtered through a 70 μM cell strainer (Greiner Bio-One cat# 542170) and spun down through a 4% BSA/DMEM-F12 solution (500 RPM, 23 degrees, 5 mins) to form a pellet. The pellet was resuspended and dispersed in 100 μL of DMEM-F12-containing growth medium. The dissociated neurons were plated onto 15 mm coverslips coated with PDL/Laminin (Neuvitro cat# GG -15-Laminin) and left in an incubator (37°C, 5% CO_2, 1.5 hr) to promote their adherence to the coverslip, after which they were flooded with 1 mL DMEM-F12 media.

2.5 Fura-2 Ca^{2+} imaging.

As previously (Milanick et al., 2019; Ostrowski et al., 2017), cells were loaded (30 min) with 1 μM Fura-2 AM calcium indicator (Invitrogen cat# F1221) in 1 mL of DMEM-F12 media with 0.01% Pluronic F-127 (Sigma cat# P2443). Following a 10 min wash in extracellular solution (ECS; 136 mM NaCl, 5.4 mM KCl, 1 mM $MgCl_2$ + 6 H_2O, 0.33 mM NaH_2PO_4, 10 mM Hepes, 10 mM D-Glucose, 2 mM $CaCl_2$ + 2 H_2O), coverslips were placed in a superfusion chamber on an Olympus IX71 microscope. All imaging protocols were carried out in ECS with the exception of the 0 mM Ca^{2+} solution, in which calcium was replaced with Mg^{2+} to a final concentration of 2.8 mM. Fura-2 was excited at 340 and 380 nm (Till Photometrics) while emission was monitored at 520 nm via a 20X water objective and Retiga Exi CCD camera. Hardware control occurred using μManager 2.0 software. Image J was used to determine the ratio between 340 and 380 nm for every given cell and these values were inputted into Excel spreadsheets for further analyses.

2.6 Drugs.

The concentrations of TRPM3 agonists Pregnenolone sulfate sodium salt (Tocris cat# 5376) and CIM 0216 (Tocris cat# 5521), and the TRPM3 antagonist Ononetin (Tocris cat# 5143), were based on previous studies (Held et al., 2015; Ragozzino et al., 2021; Straub et al., 2013). TRPM3 agonists and antagonists were initially dissolved in DMSO and subsequently diluted in ECS recording solution. Control (vehicle) experiments consisted of comparable volumes of DMSO alone added to ECS. As shown in the representative timeline (Figure 1A), following a 2 min period in ECS to establish baseline fluorescence, and agonists were applied (~60s) followed by another 300s (5 min) washout and subsequent ~60s agonist repeat. In antagonist blocking studies, ECS was applied for 120s to establish baseline fluorescence after which agonist was applied as above. After washout (240s), ononetin alone was applied for 60s followed by the addition of agonist in the presence of antagonist for an additional 75s (Figure 2A).

2.7 RNAScope.

RNAScope tests were performed using the RNAscope Multiplex Fluorescent Reagent Kit v2 (ACD biotechne Cat# 323100), and the corresponding protocols provided by the

Author Manuscript Author Manuscript Author Manuscript Author Manuscript

manufacturer. Briefly, rat nodose ganglia were collected and fixed in 4% paraformaldehyde (PFA) for 24 hours at 4 °C. Ganglia were subsequently transferred to 10%, 20% and 30% sucrose in PBS (4 °C) prior to freezing in Optimal Cutting Temperature (OCT) material on dry ice. Tissue was then cut into 17 μm sections using a cryostat (Leica), mounted on Super Frost Plus slides (Fisher Scientific cat# 12-550-15) and air dried. Following a PBS wash (5 mins), tissue was baked onto the slide (30 mins, 60 °C), immersed in 4% PFA (15 mins, 4 °C), and dehydrated in successive 50%, 70% and 100% ethanol. Slides were incubated in RNAscope Hydrogen Peroxide (10 min, 22 °C), and then rinsed 2X in dH_2O. Following target retrieval, a probe for TRPM3 mRNA (cat# 1000951-C1), or positive and negative control probes, were applied to the slides, which were then placed in the HybEZ II Oven (2 hrs, 40 °C), followed by a final rinse in Wash Buffer. Slides were stored overnight in 5X Saline Sodium Citrate (22 °C). The next day slides were washed in 1X Wash Buffer for 2 min. RNAscope Multiplex FL v2 Amp 1 and Amp 2 were added to the slides individually and baked in the HybEZ Oven (30 mins, 40° C) whereas Multiplex FL v2 Amp 3 was added to the slides and baked for 15 min at 40°C. RNAscope Multiplex v2 HRP-C1 followed by Opal 520 was used to identify *trpm3* mRNA. HRP-C2 with Opal 570 and HRP-C3 with Opal 690 were used for the positive and negative control slides. DAPI was added to cover the slides followed by addition ProLong Gold Antifade reagent (Invitrogen cat# P36930). The slides were dried overnight in the dark. Image stacks at 0.5 μm traversing the depth of the ganglia sections were acquired using an Olympus fluorescent microscope at 20X magnification. FIJI ImageJ was used to acquire Z-projection of mean and max intensity of images, and Cell Profiler 4.2.5 was used to detect and quantify the mRNA throughout the entire ganglia. The average number of *trpm3* transcripts per animal were normalized to tissue area.

2.8 RT-PCR.

Rats underwent 24-hr normoxia, 24-hr SH, 10-day normoxia or 10d CIH as described in previously, and nodose were extracted and frozen until used. mRNA was isolated via RNAqueous Total RNA Isolation Kit (Invitrogen cat# AM1931), after which cDNA was generated from 100 ng mRNA via SuperScript III First-Strand Synthesis SuperMix (Invitrogen cat# 18080-400). Real time PCR occurred via *trpm3* and *gapdh* primers (TRPM3 Fw CACGTGCAGCCAGATGTTAC, TRPM3 Rv GAACTCCAAGCTGAGAATTGAAG, GAPDH Fw TGCCCCCATGTTTGTGATG, GAPDH Rv GCTGACAATCTTGAGGGAGTTGT (0.5 μM) and 1 μL of cDNA using PowerUp SYBR Green Master Mix (Applied Biosystems cat# A25741) in an Eppendorf Smartcycler (Eppendorf). As a negative control, a series of PCR occurred with no primer or template. *trpm3* mRNA was normalized to *gadph* using the $2^{\Delta\Delta CT}$ method (Livak et al., 2001).

2.9 Analysis and Statistics.

The magnitude of Ca^{2+} response to drugs was determined using ImageJ and Microsoft Excel software. Within each agonist period, the peak 340/380 ratio was measured and reported as the change from the preceding baseline (ΔF) and plotted as (ΔF/F) with changes presented as originating from “1”. Using the normalized data, the number and magnitude of increase of responding neurons (i.e., responders) was determined by the number of neurons whose ΔF/F

Author Manuscript Author Manuscript Author Manuscript Author Manuscript

increased greater than its equivalent mean vehicle response. Graphpad Prism v9 software was used to determine normality and statistical significance, which was set at $p < 0.05$. The differences between drug or groups were determined via Mann-Whitney, Wilcoxon or Kruskal-Wallis with Dunn's tests as denoted in the text. Analysis for RNAScope and RT-PCR was performed in Excel, with the latter *trpm3* expression normalized to normoxia (plotted 1) and examined by t-test. All data shown are mean ± SEM and individual neurons.

3. RESULTS

3.1 Activation of TRPM3 channels elevate intracellular calcium.

TRPM3 channels have been shown to be expressed and active in cultured nodose neurons using Fura-2 Ca^{2+} imaging and the application of pregnenolone sulfate (Preg) (Ragozzino et al., 2021). To confirm the activity of TRPM3 channels in our neuronal cultures, Preg was perfused onto the neurons while monitoring 340/380 fluorescence ratio for each cell (Fig 1A, top). Examination of fluorescence over time in the absence of Preg served as a time control (i.e., vehicle (Veh), Fig 1A, bottom). As shown in the representative neurons (Fig 1B–D), application of 30 and 100 μM Preg reversibly increased intracellular Ca^{2+}.

To quantify the magnitude of Preg-induced Ca^{2+} elevation, we compared the responses to Preg to those of its vehicle. Across our sample, vehicle alone applied twice in succession did not increase Ca^{2+} compared to their preceding baselines (Fig 1E, Veh-1, 1.015 ± 0.006 and Veh-2, 1.025 ± 0.008). Conversely, application of Preg elevated Ca^{2+} from Bsl; those neurons that responded to Preg greater than Veh alone were categorized as "responders". Compared to Veh, Preg significantly elevated Ca^{2+} (Fig 1F, $p < 0.05$ vs Veh, Mann-Whitney test). However, between both concentrations, the increase in Ca^{2+} was similar (Fig 1F, 30 *vs.* 100 μM, $p > 0.05$, Wilcoxon test), as well as the proportion of responders (51% vs 55%).

Pregnenolone sulfate may have off-target effects (Adamusova et al., 2013). To further confirm Preg specificity as well as TRPM3-induced Ca^{2+} elevation, we performed two additional protocols. First, we examined the ability of the TRPM3 blocker ononetin (Straub et al., 2013) to prevent Preg-induced influx (timeline shown in Fig 2A). As shown in the representative cells in Fig 2B, Preg (50 μM, a dose chosen due to the similar Ca^{2+} responses with 30 and 100 μM) reversibly elevated Ca^{2+} compared to Veh ($p < 0.05$, Mann-Whitney test). Following Preg-washout, application of ononetin alone (20 μM, 60s) did not alter Ca^{2+} (340/380 ratio in ECS, 0.1762 ± 0.0167 *vs.* ONO, 0.1757 ± 0.0167, n= 46, $p > 0.05$, Wilcoxon matched-pairs signed rank test). However, ononetin eliminated the response to subsequent Preg. Quantitative data illustrating the reduction in Preg-mediated Ca^{2+} increases by TRPM3 block is shown in Fig 2C ($p < 0.05$ vs previously applied 50 μM Preg, Wilcoxon matched-pairs signed rank test). Second, we examined the Ca^{2+} response to the unique TRPM3 agonist, CIM 0216 (10, 20, and 50 μM, 60s). CIM 0216 at 20 and 50 μM significantly increased Ca^{2+} compared to vehicle and this was concentration dependent (Kruskal-Wallis test with Dunn's multiple comparison test, Fig 2D). The elevation of Ca^{2+} by CIM 0216 at 50 μM similar to that of 30 μM Preg ($p > 0.05$, Mann Whitney test, Fig 2E), suggesting maximal activation under both agonists. Taken together, these data confirm the existence of TRPM3 in visceral sensory somas and their influence on Ca^{2+} elevation.

Author Manuscript Author Manuscript Author Manuscript Author Manuscript

3.2 Pregnenolone sulfate increases Ca^{2+} signaling through membrane bound TRPM3 channels.

Functionally, our data confirm TRPM3 channels are present on the membrane of nodose neurons. TRP channels may also influence intracellular Ca^{2+} via other mechanisms including from intracellular stores (Islam, 2020). To confirm the former, Preg was applied to cells bathed in a solution lacking extracellular Ca^{2+} (0 mM, 60s). The addition of Preg in a 0 mM Ca^{2+} solution ablated the increase in intracellular Ca^{2+}. Comparing the 30 and 100 μM Preg response in normal 2 mM Ca^{2+} to those in 0 mM Ca^{2+} confirmed a significantly attenuated response ($p < 0.05$, Mann-Whitney test, Fig 2F). These data indicate activation of TRPM3 induces Ca^{2+} influx through membrane-bound channels.

3.3 Acute in vivo sustained hypoxia enhances TRPM3 Ca^{2+} response, which is reversible following recovery.

Exposure to acute sustained hypoxia (SH, 10% O_2) induces cardiorespiratory plasticity including enhanced peripheral reflex sensitivity and nTS activity (Matott et al., 2020). Hypoxia also contributes to or is associated with altered TRP channels (Kline et al., 2019). To examine if acute *in vivo* SH altered TRPM3 function, we subjected rats to either room air (21% O_2) or 10% inspired O_2 for 24hr followed by neuronal examination as Fig 1 and 2. Vehicle was again without effect on Ca^{2+} following *in vivo* hypoxia or normoxia (not shown). As quantified in Fig 3A, Preg (30 μM) increased intracellular Ca^{2+} to a greater extent after *in vivo* 24-hr hypoxia compared to *in vivo* 24-hr Norm exposure ($p < 0.05$, Kruskal-Wallis with Dunn's test). The greater increase in Ca^{2+} after hypoxia occurred despite the similar number of cells that respond to Preg in Norm and hypoxia (43% *vs*. 40%, respectively).

The magnitude by which *in* vivo SH exposure irreversibly altered TRPM3 function was next examined. To test the potential reversibility of exaggerated Ca^{2+} responses to TRPM3 activation after *in vivo* SH, rats were exposed to 24-hr SH followed by 24-hr normoxic exposure. As a time control, another group of rats was exposed to persistent 48-hr normoxia. Following neuronal dissociation, 30 μM Preg was applied as Figure 1. Preg increased intracellular Ca^{2+} the same degree after 24-hr SH + 24-hr Norm (n= 61) as their 48-hr Norm controls (n= 45, $p > 0.05$, Kruskal-Wallis with Dunn's test, Fig 3A). Importantly, responses to TRPM3 activation after 24-hr SH was greater than that of 48-hr Norm and 24-hr SH + 24-hr Norm ($p < 0.05$ vs 24-hr SH alone, Fig 3A), demonstrating reversibility of effects.

3.4 In vitro hypoxia does not elevate TRPM3 responses.

In vivo hypoxia results in cardiorespiratory adjustments due to neuronal activity and hypoxic exposure. We sought to determine if acute sustained *in vitro* hypoxia alters TRPM3-induced Ca^{2+} responses to Preg (30 μM), independent of the (neuro)physiological effects. Here, following isolation of neurons from naïve rodents, cultures were exposed to either 24-hr of 1% O_2 or as a control 21% O_2 (i.e., Norm). As above, cells were exposed to either Preg or vehicle with the latter responses again serving to set the threshold for consideration of a Preg-response. As quantified in Figure 3B, although the number, or distribution, of neurons that responded to Preg tended to be greater after *in vitro* SH ($p = 0.07$, Kolmogorov-Smirnov test), the overall magnitude was similar in extent to *in vitro* Norm ($p = 0.14$,

Author Manuscript Author Manuscript Author Manuscript Author Manuscript

Mann Whitney). The number of responders was also similar (Norm, 59% vs hypoxia, 56%). Together, these data suggest that reduced oxygen tension alone does not increase TRPM3 function in nodose neurons.

3.5 Chronic intermittent hypoxic exposure does not elevate TRPM3 Ca^{2+} response.

To examine if the pattern of hypoxic exposure is critical for TRPM3-altered function (Prabhakar et al., 2002), we examined neurons following *in vivo* chronic intermittent hypoxia (CIH), which mimics episodic breathing in a variety of conditions. We have shown that CIH alters TRPV1 expression and function to contribute to altered afferent signaling (Kline et al., 2019). In the present study, rats were exposed to 10 days CIH during their inactive period as per our previous studies (Kline et al., 2009; Kline et al., 2007; Kline et al., 2019). Neuronal dissociation and Preg application occurred the following day, a time frame within which nTS synaptic alterations persist after CIH. In contrast to SH, the magnitude of Preg-induced calcium influx was similar between Norm and CIH ($p = 0.17$, Mann-Whitney test, Fig 3C) exposed neurons.

3.6 Trpm3 mRNA expression increases after hypoxia.

The expression of *trpm3* mRNA following SH was examined via RNAScope. As shown in Fig 4A, *trpm3* was expressed in neurons throughout the normoxic and SH nodose ganglion. Quantifying expression demonstrated a significant elevation of mRNA transcript after SH (n=3 each, $p < 0.05$, Fig 4B). RT-PCR analysis demonstrated that SH tended to elevate *trpm3* expression relative to their normoxic controls (SH, Fig 4C, n= 5–6 ea, $p = 0.086$). Exposure to CIH also significantly elevated TRPM3 mRNA compared to their matched normoxic controls (Fig 4D, n=4 ea, $p < 0.05$).

4. DISCUSSION

In the present study, we confirmed TRPM3 is localized and functional within the rat nodose ganglia. When activated these channels increase intracellular Ca^{2+} via transmembrane influx. We further demonstrate SH exposure increases the Ca^{2+} response to TRPM3 activation and this augmentation occurred following in vivo, but not in vitro, sustained hypoxia exposure. The hypoxia-induced elevation in response to TRPM3 activation is reversible following return to normoxia. By contrast, CIH did not alter Ca^{2+} responses to TRPM3 activation. Taken together, these studies provide a potential role of TRPM3 in the hypoxia-induced altered vagal reflex sensitivity.

TRP channels are expressed within peripheral viscero- and chemosensory afferents, their central nTS processes, and are functionally relevant. For instance, members of the vanilloid family TRPV1-4 (Fenwick et al., 2014; Gu et al., 2005; Okano et al., 2006; Sasaki et al., 2013; Wu et al., 2016; Yamamoto et al., 2007; Zhang et al., 2004) and ankyrin family TRPA1 (Brierley et al., 2009; Choi et al., 2011; Hondoh et al., 2010; Sun et al., 2020; Zhao et al., 2010) have been localized to ganglia neurons. TRPA1 participates in enhancing nTS discharge in response to lung irritants (Mutoh et al., 2013) and increases nTS synaptic activity via their presynaptic contribution (Feng et al., 2019). Members of the TRPC (canonical) family are found within the carotid body and its innervating petrosal ganglia

Author Manuscript Author Manuscript Author Manuscript Author Manuscript

neurons (Buniel et al., 2003). Of the TRPM (melastatin) family, TRPM3, 7 & 8 are found in the carotid body (Shin et al., 2019) and petrosal ganglia neurons (Hondoh et al., 2010; Hossain et al., 2018; Nassenstein et al., 2008; Yajima et al., 2019; Yu et al., 2015; Zhang et al., 2004; Zhao et al., 2010). Relevant to the present study, TRPM3 has also been localized within nodose ganglion neurons. TRPM3 increases in expression during development (Staaf et al., 2010). In the juvenile rat, TRPM3 mRNA and protein are expressed in 24 –76% (Jawaid et al., 2022; Ragozzino et al., 2021) of nodose neurons. Confocal analysis further suggests that of those 24% of cells that have high expression of TRPM3, localization is below or near the surface of the membrane (Jawaid et al., 2022). Our studies using RNAScope analysis confirm robust mRNA of TRPM3 in the nodose ganglia, yet whether its mRNA expression represents high or low protein requires further analysis.

Our results further confirm the functional relevance of TRPM3 in vagal neurons. Bath application of the TRPM3 agonist pregnenolone reversibly increased intracellular Ca^{2+} via transmembrane influx, consistent with previous studies in the nodose (Ragozzino et al., 2021) and other sensory neurons (Thiel et al., 2017). While pregnenolone is a prototypic TRPM3 agonist, it may possess off-target effects (Thiel et al., 2017). To confirm the activation of TRPM3 channels by pregnenolone, we applied the specific TRPM3 channel blocker ononetin along with pregnenolone and noted ablation of the response. In addition, pregnenolone had no effect on calcium influx in TRPM3 knockout mice (Ragozzino et al., 2021). Last, the use of an additional TRPM3-specific agonist (CIM 0216) mimicked the Ca^{2+} increase caused by pregnenolone. Overall, activation of TRPM3 increased Ca^{2+} in a large proportion, but not all, of the neurons studied confirming that not all vagal afferent express functional TRPM3. Alternatively, those neurons that express TRPM3 yet do not functionally increase Ca^{2+} upon their activation may represent those neurons that express splice variants that have less Ca^{2+} permeability (Thiel et al., 2017).

Exposure to hypoxia is a common stressor that results in and is associated with elevated chemoreflex and altered autonomic function. In this study, we examined the potential role for TRPM3 in vagal afferent responses following sustained and intermittent hypoxia. Exposure to acute sustained hypoxia (SH) decreases baroreflex control of heart rate and induces tachycardia, effects mediated in part through the vagus. We and others have shown that one day of SH enhances nTS glutamatergic synaptic transmission within the nTS via presynaptic mechanisms (Accorsi-Mendonca et al., 2015; Accorsi-Mendonca et al., 2019; Matott et al., 2020), which may be due, in part, to sensitization of the central afferent synapses (Flor et al., 2018). Given the importance of TRPM3 to elevate nTS glutamatergic neurotransmission (Ragozzino et al., 2021), we sought to examine the elevation of Ca^{2+} following activation of these channels in sensory somas. Following 24-hr of SH exposure (10% O_2), activation of TRPM3 channels increased Ca^{2+} significantly more than their normoxic controls. However, the number of responders remained constant between the SH and their normoxic control group. Importantly, these enhanced Ca^{2+} responses readily reversed following an additional 24-hr of normoxic exposure. While we did not evaluate TRPM3 protein expression, mRNA expression was elevated by SH when examined via RNAScope. Although our RT-PCR analysis of SH versus Norm mRNA did not reach statistical significance, the results were consistent with that of RNAScope. The increase in mRNA when measured by RT-PCR may be limited by differences in ganglia isolation

Author Manuscript Author Manuscript Author Manuscript Author Manuscript

or cDNA generation, compared to the direct binding of RNAScope in tissue. Overall, the augmented Ca^{2+} responses may suggest increased conduction through the TRPM3 channel as well as a potential increase in expression after hypoxia.

In vivo hypoxia elevates neuronal and humoral/neuropeptide activity (Chen et al., 2007; Goraca, 2004; Kelestimur et al., 1997; Ruyle et al., 2018; Stegner et al., 1984) that may influence TRPM3 function via the influence of one or more second messengers (Thiel et al., 2017). To minimize the potential influence of neuronal and humoral activity in our interpretation, we examined Ca^{2+} responses following in vitro hypoxia. To do so, following their dissociation, nodose neurons were placed in a sealed chamber containing 1% O_2-5% CO_2 or 21% O_2-5% CO_2 (normoxic controls). TRPM3 activation tended to but did not statistically enhance the Ca^{2+} response, or their distribution, after *in vitro* hypoxic exposure compared to their normoxic controls. Although we set the oxygen concentration to 1%, a common level for *in vitro* hypoxic exposure studies (Wu et al., 2011) including those examining TRP channels (Parpaite et al., 2016), we do not know the partial pressure of oxygen (pO2) within the media nor whether it remained consistent for the entirety of exposure (Pavlacky et al., 2020). It may also be more hypoxic than that during *in vivo* exposure. It is likely that pO_2 within the ganglia tissue is considerably lower than the inspired 10% O_2 due to tissue metabolism. For instance, while the pO_2 within the nodose is unknown, the mean pO_2 of the rat dorsal root ganglia is ~36 torr while inspiring room air (Zochodne et al., 1991), and likely even lower under hypoxic conditions. Thus, shorter or longer in vitro SH may have greater effects. Nevertheless, our data showing exposure to *in vivo*, but not *in vitro*, sustained hypoxia augments TRPM3-mediated calcium influx suggested the increase in function may be due to neuronal activity-dependent changes that occur in hypoxia.

In contrast to sustained hypoxia, TRPM3 function was not altered following 10 days of CIH that mimics the brief (~ 45s) hypoxic episodes observed during sleep apnea. We had hypothesized CIH would elevate TRPM3 expression and/or function given its contribution to nTS signaling (Ragozzino et al., 2021) and the CIH elevation of spontaneous glutamate release due in part to increased TRPV1 function (Kline et al., 2019). TRPM3 continued to influence nodose activity in ~ 50% of neurons, yet the magnitude of response was not altered compared to normoxic rats. These data further indicate that the pattern of in vivo neuronal activity or hypoxic exposure is critical to the influence on TRPM3 on Ca^{2+} influx. In particular, we demonstrate the increased TRPM3 function following SH is reversed after a 24-hr return to normal oxygen levels. Given that we monitored TRPM3-mediated Ca^{2+} elevation ~ 12 hrs after the last hypoxic bout during the CIH exposure, any functional increase may have quickly reversed. The prolonged resting period between the last hypoxic bout and recording may also contribute to the discrepancy between the *trpm3* mRNA elevation in CIH yet lack of functional effects. Interestingly, a similar time course does not reverse many of the CIH-induced changes in synaptic neurotransmission at the sensory afferent-nTS synapse (Kline et al., 2009; Kline et al., 2007; Kline et al., 2019).

Sustained hypoxia may directly influence TRPM3 channel activity as it does for other members of the TRP family. For instance, overnight exposure to hypoxia sensitizes TRPV1 in HEK293T cells and rat sensory neurons, increasing inward current amplitude in response

Author Manuscript Author Manuscript Author Manuscript Author Manuscript

to capsaicin (Kim et al., 2012; Ristoiu et al., 2011), and TRPA1 and TRPM7 have been suggested to be O_2 sensors (Mori et al., 2017). Such elevation in current may be due, in part to changes in redox state or activation of hypoxia-inducible factor (HIF) to elevate signaling cascades (Hatano et al., 2021; Nagarajan et al., 2017). In addition, elevation of transcription factors such as cFos and AP-1 in response to hypoxia (Premkumar et al., 2000) and/or TRPM3 activation (Thiel et al., 2017), may influence expression or function of one or more crucial proteins. Hypoxia may also alter G-protein-coupled receptors. For instance, activation of Gβγ subunits reduce TRPM3 activity whereas phosphoinositide phosphoinositol 4,5-biphosphate (PI(4,5)P2) enhances its activity (Vriens et al., 2018). It is tempting to speculate that an altered balance between these systems may enhance TRPM3 function, in addition to expression, following SH.

In conclusion, TRPM3 channels are expressed in the nodose ganglion and increase calcium-influx following hypoxia. The increase in TRPM3 function was hypoxic specific and reversed by 24 hours of normal oxygen levels following the removal of the hypoxic stimulus. These results may suggest TRPM3 channels contribute to reflex function.

ACKNOWLEDGEMENTS

We thank Dr. Luis Polo-Parada for use of laboratory equipment. This study was supported by HL128454 & HL098602 (DDK)

ABBREVIATIONS

Ca^{2+}	Calcium
CIH	Chronic intermittent hypoxia
Norm	Normoxia
nTS	Nucleus Tractus Solitarii
O_2	Oxygen
Preg	Pregnenolone sulfate
SH	Sustained hypoxia
TRPM3	Transient receptor potential cation channel subfamily M member 3

6. REFERENCES

Accorsi-Mendonca D, Almado CE, Bonagamba LG, Castania JA, Moraes DJ, Machado BH 2015. Enhanced Firing in NTS Induced by Short-Term Sustained Hypoxia Is Modulated by Glia-Neuron Interaction. J Neurosci 35, 6903–6917. [PubMed: 25926465]

Accorsi-Mendonca D, Bonagamba LG, Machado BH 2019. Astrocytic modulation of glutamatergic synaptic transmission is reduced in NTS of rats submitted to short-term sustained hypoxia. J Neurophysiol.

Adamusova E, Cais O, Vyklicky V, Kudova E, Chodounska H, Horak M, Vyklicky L Jr. 2013. Pregnenolone sulfate activates NMDA receptor channels. Physiol Res 62, 731–736. [PubMed: 24359434]

Author Manuscript Author Manuscript Author Manuscript Author Manuscript

Brierley SM, Hughes PA, Page AJ, Kwan KY, Martin CM, O'Donnell TA, Cooper NJ, Harrington AM, Adam B, Liebregts T, Holtmann G, Corey DP, Rychkov GY, Blackshaw LA 2009. The ion channel TRPA1 is required for normal mechanosensation and is modulated by algesic stimuli. Gastroenterology 137, 2084–2095 e2083. [PubMed: 19632231]

Buniel MC, Schilling WP, Kunze DL 2003. Distribution of transient receptor potential channels in the rat carotid chemosensory pathway. J Comp Neurol 464, 404–413. [PubMed: 12900933]

Chen S, Takahashi N, Chen C, Pauli JL, Kuroki C, Kaminosono J, Kashiwadani H, Kanmura Y, Mori Y, Ou S, Hao L, Kuwaki T 2020. Transient Receptor Potential Ankyrin 1 Mediates Hypoxic Responses in Mice. Front Physiol 11, 576209. [PubMed: 33192579]

Chen XQ, Dong J, Niu CY, Fan JM, Du JZ 2007. Effects of hypoxia on glucose, insulin, glucagon, and modulation by corticotropin-releasing factor receptor type 1 in the rat. Endocrinology 148, 3271–3278. [PubMed: 17379644]

Choi MJ, Jin Z, Park YS, Rhee YK, Jin YH 2011. Transient receptor potential (TRP) A1 activated currents in TRPV1 and cholecystokinin-sensitive cranial visceral afferent neurons. Brain Res 1383, 36–42. [PubMed: 21316356]

Dantzler HA, Kline DD 2020. Exaggerated potassium current reduction by oxytocin in visceral sensory neurons following chronic intermittent hypoxia. Auton Neurosci 229, 102735. [PubMed: 33032244]

Feng L, Uteshev VV, Premkumar LS 2019. Expression and Function of Transient Receptor Potential Ankyrin 1 Ion Channels in the Caudal Nucleus of the Solitary Tract. Int J Mol Sci 20.

Fenwick AJ, Wu S-W, Peters JH 2014. Isolation of TRPV1 independent mechanisms of spontaneous and asynchronous glutamate release at primary afferent to NTS synapses. Frontiers in Neuroscience 8, 6. [PubMed: 24550768]

Flor KC, Silva EF, Menezes MF, Pedrino GR, Colombari E, Zoccal DB 2018. Short-Term Sustained Hypoxia Elevates Basal and Hypoxia-Induced Ventilation but Not the Carotid Body Chemoreceptor Activity in Rats. Front Physiol 9, 134. [PubMed: 29535636]

Goraca A 2004. Oxytocin content in the venous blood outflowing from the vicinity of the cavernous sinus and from the femoral vein. Endocrine Regulations 38, 119–125. [PubMed: 15693290]

Gu Q, Lin RL, Hu HZ, Zhu MX, Lee LY 2005. 2-aminoethoxydiphenyl borate stimulates pulmonary C neurons via the activation of TRPV channels. Am J Physiol Lung Cell Mol Physiol 288, L932–941. [PubMed: 15653710]

Hatano N, Matsubara M, Suzuki H, Muraki Y, Muraki K 2021. HIF-1alpha Dependent Upregulation of ZIP8, ZIP14, and TRPA1 Modify Intracellular Zn(2+) Accumulation in Inflammatory Synoviocytes. Int J Mol Sci 22.

Held K, Kichko T, De Clercq K, Klaassen H, Van Bree R, Vanherck JC, Marchand A, Reeh PW, Chaltin P, Voets T, Vriens J 2015. Activation of TRPM3 by a potent synthetic ligand reveals a role in peptide release. Proc Natl Acad Sci U S A 112, E1363–1372. [PubMed: 25733887]

Hondoh A, Ishida Y, Ugawa S, Ueda T, Shibata Y, Yamada T, Shikano M, Murakami S, Shimada S 2010. Distinct expression of cold receptors (TRPM8 and TRPA1) in the rat nodose-petrosal ganglion complex. Brain Res 1319, 60–69. [PubMed: 20079339]

Hossain MZ, Ando H, Unno S, Masuda Y, Kitagawa J 2018. Activation of TRPV1 and TRPM8 Channels in the Larynx and Associated Laryngopharyngeal Regions Facilitates the Swallowing Reflex. Int J Mol Sci 19.

Islam MS 2020. Molecular Regulations and Functions of the Transient Receptor Potential Channels of the Islets of Langerhans and Insulinoma Cells. Cells 9.

Jawaid S, Herring AI, Getsy PM, Lewis SJ, Watanabe M, Kolesova H 2022. Differential immunostaining patterns of transient receptor potential (TRP) ion channels in the rat nodose ganglion. J Anat 241, 230–244. [PubMed: 35396708]

Kelestimur H, Leach RM, Ward JPT, Forsling ML 1997. Vasopressin and oxytocin release during prolonged environmental hypoxia in the rat. Thorax 52, 84–88. [PubMed: 9039242]

Kim KS, Yoo HY, Park KS, Kim JK, Zhang YH, Kim SJ 2012. Differential effects of acute hypoxia on the activation of TRPV1 by capsaicin and acidic pH. J Physiol Sci 62, 93–103. [PubMed: 22215506]

Author Manuscript Author Manuscript Author Manuscript Author Manuscript

Kline DD, Hendricks G, Hermann G, Rogers RC, Kunze DL 2009. Dopamine inhibits N-type channels in visceral afferents to reduce synaptic transmitter release under normoxic and chronic intermittent hypoxic conditions. J Neurophysiol 101, 2270–2278. [PubMed: 19244351]

Kline DD, Ramirez-Navarro A, Kunze DL 2007. Adaptive depression in synaptic transmission in the nucleus of the solitary tract after in vivo chronic intermittent hypoxia: evidence for homeostatic plasticity. J.Neurosci. 27, 4663–4673. [PubMed: 17460079]

Kline DD, Wang S, Kunze DL 2019. TRPV1 channels contribute to spontaneous glutamate release in nucleus tractus solitarii following chronic intermittent hypoxia. J Neurophysiol 121, 881–892. [PubMed: 30601692]

Kupari J, Haring M, Agirre E, Castelo-Branco G, Ernfors P 2019. An Atlas of Vagal Sensory Neurons and Their Molecular Specialization. Cell Rep 27, 2508–2523 e2504. [PubMed: 31116992]

Livak KJ, Schmittgen TD 2001. Analysis of relative gene expression data using real-time quantitative PCR and the 2(-Delta Delta C(T)) Method. Methods (San Diego, Calif.) 25, 402–408. [PubMed: 11846609]

Matott MP, Hasser EM, Kline DD 2020. Sustained Hypoxia Alters nTS Glutamatergic Signaling and Expression and Function of Excitatory Amino Acid Transporters. Neuroscience 430, 131–140. [PubMed: 32032667]

Milanick WJ, Polo-Parada L, Dantzler HA, Kline DD 2019. Activation of alpha-1 adrenergic receptors increases cytosolic calcium in neurones of the paraventricular nucleus of the hypothalamus. J Neuroendocrinol 31, e12791. [PubMed: 31494990]

Min S, Chang RB, Prescott SL, Beeler B, Joshi NR, Strochlic DE, Liberles SD 2019. Arterial Baroreceptors Sense Blood Pressure through Decorated Aortic Claws. Cell Rep 29, 2192–2201 e2193. [PubMed: 31747594]

Mori Y, Takahashi N, Kurokawa T, Kiyonaka S 2017. TRP channels in oxygen physiology: distinctive functional properties and roles of TRPA1 in O2 sensing. Proc Jpn Acad Ser B Phys Biol Sci 93, 464–482.

Mutoh T, Taki Y, Tsubone H 2013. Desflurane but not sevoflurane augments laryngeal C-fiber inputs to nucleus tractus solitarii neurons by activating transient receptor potential-A1. Life Sci 92, 821–828. [PubMed: 23499557]

Nagarajan Y, Rychkov GY, Peet DJ 2017. Modulation of TRP Channel Activity by Hydroxylation and Its Therapeutic Potential. Pharmaceuticals (Basel) 10.

Nassenstein C, Kwong K, Taylor-Clark T, Kollarik M, Macglashan DM, Braun A, Undem BJ 2008. Expression and function of the ion channel TRPA1 in vagal afferent nerves innervating mouse lungs. J Physiol 586, 1595–1604. [PubMed: 18218683]

Okano H, Koike S, Bamba H, Toyoda K, Uno T, Hisa Y 2006. Participation of TRPV1 and TRPV2 in the rat laryngeal sensory innervation. Neurosci Lett 400, 35–38. [PubMed: 16517068]

Ostrowski TD, Dantzler HA, Polo-Parada L, Kline DD 2017. H2O2 augments cytosolic calcium in nucleus tractus solitarii neurons via multiple voltage-gated calcium channels. Am J Physiol Cell Physiol 312, C651–C662. [PubMed: 28274920]

Parpaite T, Cardouat G, Mauroux M, Gillibert-Duplantier J, Robillard P, Quignard JF, Marthan R, Savineau JP, Ducret T 2016. Effect of hypoxia on TRPV1 and TRPV4 channels in rat pulmonary arterial smooth muscle cells. Pflugers Arch 468, 111–130. [PubMed: 25799977]

Pavlacky J, Polak J 2020. Technical Feasibility and Physiological Relevance of Hypoxic Cell Culture Models. Front Endocrinol (Lausanne) 11, 57. [PubMed: 32153502]

Prabhakar NR, Kline DD 2002. Ventilatory changes during intermittent hypoxia: importance of pattern and duration. High Alt. Med. Biol 3, 195–204. [PubMed: 12162863]

Premkumar DR, Adhikary G, Overholt JL, Simonson MS, Cherniack NS, Prabhakar NR 2000. Intracellular pathways linking hypoxia to activation of c-fos and AP-1. Adv Exp Med Biol 475, 101–109. [PubMed: 10849652]

Ragozzino FJ, Arnold RA, Fenwick AJ, Riley TP, Lindberg JEM, Peterson B, Peters JH 2021. TRPM3 expression and control of glutamate release from primary vagal afferent neurons. J Neurophysiol 125, 199–210. [PubMed: 33296617]

Author Manuscript Author Manuscript Author Manuscript Author Manuscript

Ristoiu V, Shibasaki K, Uchida K, Zhou Y, Ton BH, Flonta ML, Tominaga M 2011. Hypoxia-induced sensitization of transient receptor potential vanilloid 1 involves activation of hypoxia-inducible factor-1 alpha and PKC. Pain 152, 936–945. [PubMed: 21376466]

Ruyle BC, Klutho PJ, Baines CP, Heesch CM, Hasser EM 2018. Hypoxia activates a neuropeptidergic pathway from the paraventricular nucleus of the hypothalamus to the nucleus tractus solitarii. American Journal of Physiology-Regulatory, Integrative and Comparative Physiology 315, R1167–R1182. [PubMed: 30230933]

Sasaki R, Sato T, Yajima T, Kano M, Suzuki T, Ichikawa H 2013. The distribution of TRPV1 and TRPV2 in the rat pharynx. Cell Mol Neurobiol 33, 707–714. [PubMed: 23584686]

Schild JH, Kunze DL 2012. Differential distribution of voltage-gated channels in myelinated and unmyelinated baroreceptor afferents. Autonomic neuroscience : basic & clinical 172, 4–12. [PubMed: 23146622]

Shin MK, Eraso CC, Mu YP, Gu C, Yeung BHY, Kim LJ, Liu XR, Wu ZJ, Paudel O, Pichard LE, Shirahata M, Tang WY, Sham JSK, Polotsky VY 2019. Leptin Induces Hypertension Acting on Transient Receptor Potential Melastatin 7 Channel in the Carotid Body. Circ Res 125, 989–1002. [PubMed: 31545149]

Shirahata M, Tang WY, Shin MK, Polotsky VY 2015. Is the Carotid Body a Metabolic Monitor? Adv Exp Med Biol 860, 153–159. [PubMed: 26303477]

Staaf S, Franck MC, Marmigere F, Mattsson JP, Ernfors P 2010. Dynamic expression of the TRPM subgroup of ion channels in developing mouse sensory neurons. Gene Expr Patterns 10, 65–74. [PubMed: 19850157]

Stegner H, Leake RD, Palmer SM, Oakes G, Fisher DA 1984. The effect of hypoxia on neurohypophyseal hormone release in fetal and maternal sheep. Pediatric Research 18, 188–191. [PubMed: 6422435]

Straub I, Mohr F, Stab J, Konrad M, Philipp SE, Oberwinkler J, Schaefer M 2013. Citrus fruit and fabacea secondary metabolites potently and selectively block TRPM3. Br J Pharmacol 168, 1835–1850. [PubMed: 23190005]

Sun H, Meeker S, Undem BJ 2020. Role of TRP channels in G(q)-coupled protease-activated receptor 1-mediated activation of mouse nodose pulmonary C-fibers. Am J Physiol Lung Cell Mol Physiol 318, L192–L199. [PubMed: 31664854]

Thiel G, Rubil S, Lesch A, Guethlein LA, Rossler OG 2017. Transient receptor potential TRPM3 channels: Pharmacology, signaling, and biological functions. Pharmacol Res 124, 92–99. [PubMed: 28720517]

Vriens J, Voets T 2018. Sensing the heat with TRPM3. Pflugers Arch 470, 799–807. [PubMed: 29305649]

Wu D, Yotnda P 2011. Induction and testing of hypoxia in cell culture. J Vis Exp.

Wu SW, Lindberg JE, Peters JH 2016. Genetic and pharmacological evidence for low-abundance TRPV3 expression in primary vagal afferent neurons. Am J Physiol Regul Integr Comp Physiol 310, R794–805. [PubMed: 26843581]

Yajima T, Sato T, Shimazaki K, Ichikawa H 2019. Transient receptor potential melastatin-3 in the rat sensory ganglia of the trigeminal, glossopharyngeal and vagus nerves. J Chem Neuroanat 96, 116–125. [PubMed: 30639448]

Yamamoto Y, Sato Y, Taniguchi K 2007. Distribution of TRPV1- and TRPV2-immunoreactive afferent nerve endings in rat trachea. J Anat 211, 775–783. [PubMed: 17979952]

Yu X, Hu Y, Ru F, Kollarik M, Undem BJ, Yu S 2015. TRPM8 function and expression in vagal sensory neurons and afferent nerves innervating guinea pig esophagus. Am J Physiol Gastrointest Liver Physiol 308, G489–496. [PubMed: 25591866]

Zhang L, Jones S, Brody K, Costa M, Brookes SJ 2004. Thermosensitive transient receptor potential channels in vagal afferent neurons of the mouse. Am J Physiol Gastrointest Liver Physiol 286, G983–991. [PubMed: 14726308]

Zhao H, Simasko SM 2010. Role of transient receptor potential channels in cholecystokinin-induced activation of cultured vagal afferent neurons. Endocrinology 151, 5237–5246. [PubMed: 20881249]

Zochodne DW, Ho LT 1991. Unique microvascular characteristics of the dorsal root ganglion in the rat. Brain Res 559, 89–93. [PubMed: 1782562]

Author Manuscript Author Manuscript Author Manuscript Author Manuscript

Author Manuscript Author Manuscript Author Manuscript Author Manuscript

HIGHLIGHTS

- Activation of TRPM3 channels in nodose neurons increases intracellular calcium
- In vivo short-sustained hypoxia (1d, 10% O_2) reversibly increases TRPM3 calcium responses
- By contrast, in vivo 10-day intermittent hypoxia did not alter TRPM3 responses
- Hypoxia increases trpm3 mRNA transcripts

Author Manuscript Author Manuscript Author Manuscript Author Manuscript

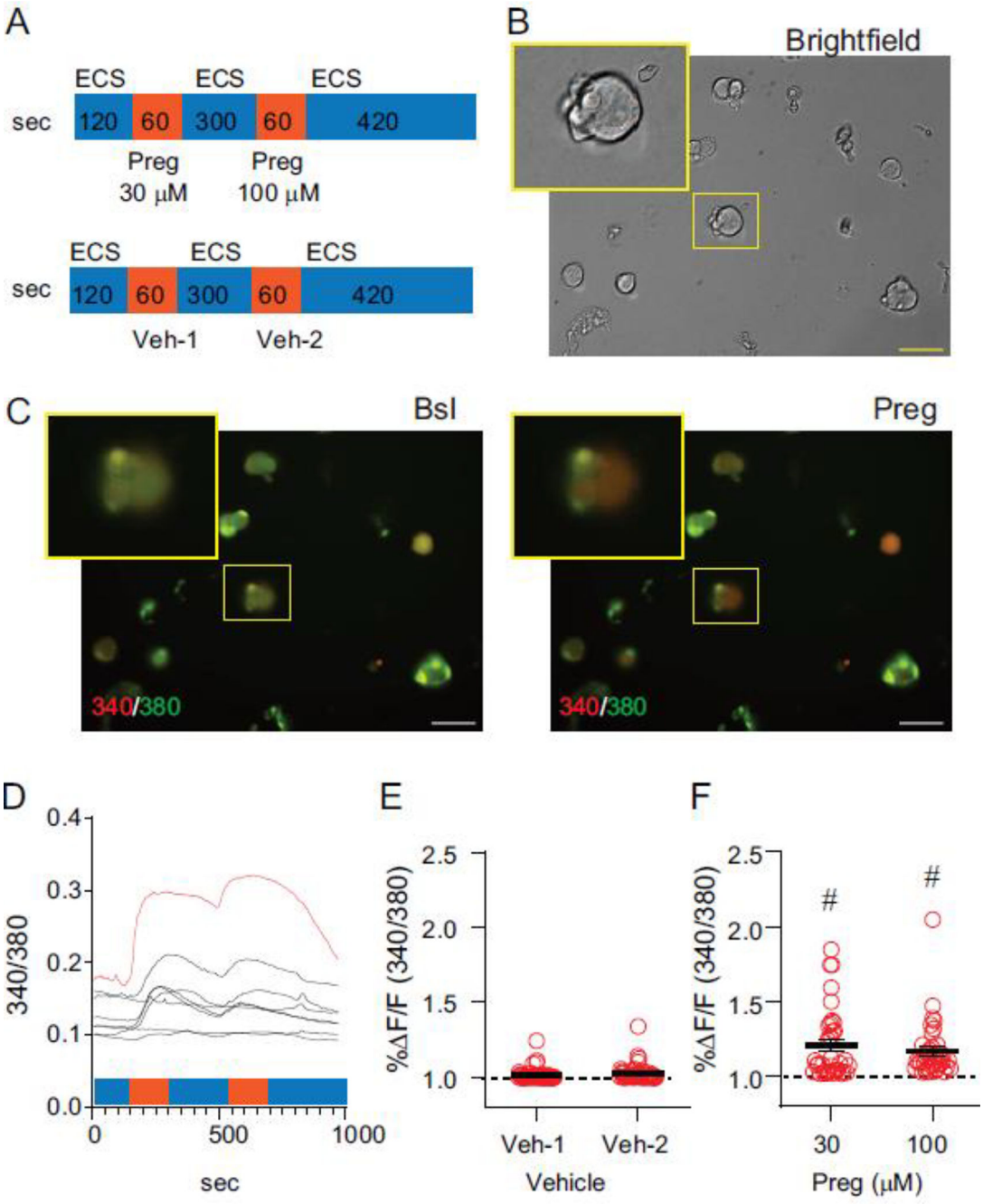

Figure 1. TRPM3 activation increases intracellular Ca^{2+}.

(A) TRPM3 agonist Pregnenolone (Preg) was applied to neurons twice at two different concentrations (60s ea.) with a wash in extracellular solution (ECS) occurring in between (300s). Vehicle experiments using an identical timeline were performed to examine Ca^{2+} changes over time. (B) Brightfield image showing acute isolated neurons. C) Fluorescence (520 nm) of neurons shown in B excited under 340 (red) and 380 (green) nm fluorescence. Shown is the overlay. Note increase in red fluorescence from Bsl after Preg is applied, indicating elevation of intracellular calcium. Insets in B,C show magnified view of

Author Manuscript Author Manuscript Author Manuscript Author Manuscript

individual cell. (D) Cells shown in C demonstrating a robust response to 30 and 100 μM Preg (orange highlight). B-C, Scale bar is 25 μM. (E, F) Ratio of 340/380 fluorescence during vehicle (E) and Preg (F) in relation to the immediate baseline prior to their application (%ΔF/F). "1" and dashed line denotes lack of change from baseline. Vehicle (E, n=48) alone did not increase Ca^{2+}, whereas Preg (F) at 30 and 100 μM (n=36 and 39, respectively) increased Ca^{2+} from their baseline which is similar between concentrations. $p > 0.05$, 30 vs 100 μM Preg, Wilcoxon matched-pairs signed rank test; #, $p < 0.05$ vs respective Veh, Mann-Whitney test.

Author Manuscript Author Manuscript Author Manuscript Author Manuscript

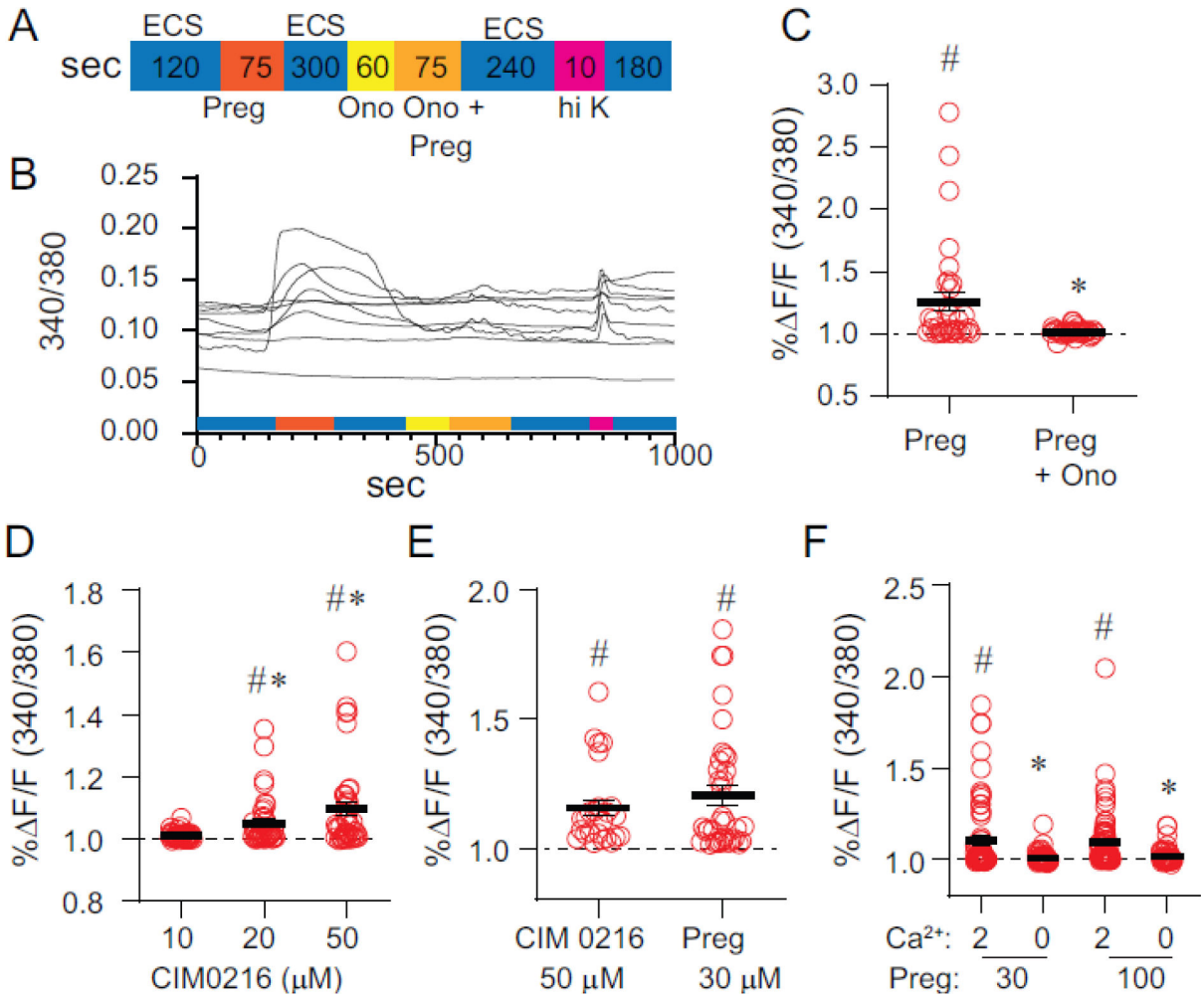

Figure 2. Confirmation of TRPM3 function in nodose neurons.

(A, B) Protocol timeline and representative examples. Preg (50 μM) was applied to neurons, demonstrating an increase in Ca^{2+}. After its wash-out, TRPM3 blocker Ononetin (Ono) was applied, followed by Preg in the presence of Ono. Note the reduction in TRPM3-mediated increase. Elevated K (50 mM, 10s) was applied to confirm the cells remained responsive after the Ono-mediated reduction in Ca^{2+}. (C) Quantitative data. Preg response is eliminated by Ono. n= 33; #, $p < 0.05$ vs Veh, Mann Whitney test; *, $p < 0.05$ vs Preg alone, Wilcoxon test. (D) As an additional test, the TRPM3 agonist, CIM0216, was applied at increasing concentrations with an intermittent washout. Neurons demonstrated an elevation of Ca^{2+} with CIM0216. n= 41; #, $p < 0.05$, CIM0216 vs Veh; *, $p < 0.05$, 20 and 50 vs 10 μM; Kruskal-Wallis test with Dunn's multiple comparison test. (E) CIM0216 and Preg produce similar magnitudes of response, $p > 0.05$, Mann Whitney test. (F) To examine the necessity for extracellular Ca^{2+} in the TRPM3-mediated increase in intracellular Ca^{2+}, Preg was applied in the absence of extracellular Ca^{2+} (balanced via an increase in Mg^{2+}). Preg at 30 and 100 μM in 0 mM calcium solution does not elicit elevation of Ca^{2+} (* $p < 0.05$ vs 2 mM Preg, #, $p < 0.05$ vs Veh, Mann-Whitney test). 0 mM Ca^{2+}, n= 52; 2 mM Ca^{2+}, n= 71.

Author Manuscript Author Manuscript Author Manuscript Author Manuscript

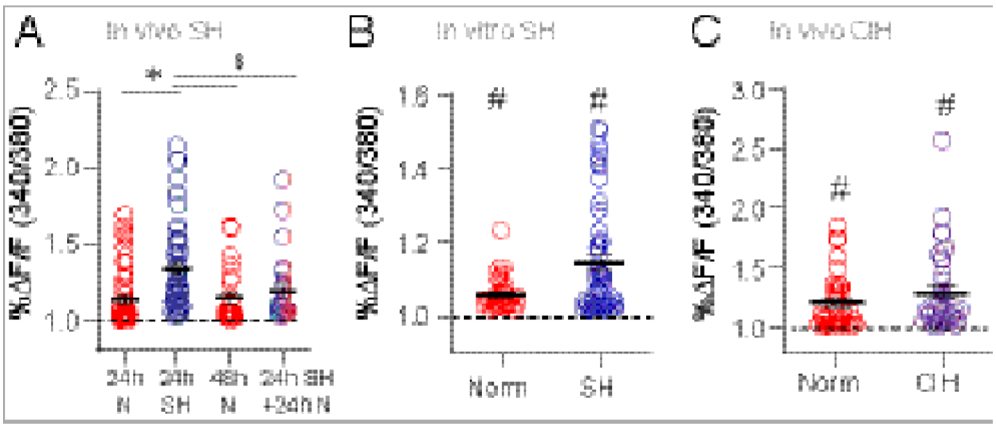

Figure 3. In vivo sustained hypoxia elevates TRPM3-mediated calcium influx.

(A) Protocol as described in Fig 1A. Preg (30 μM) increased intracellular calcium concentrations more in *in vivo* 24hr SH cells than in *in vivo* 24hr Norm (N) cells. Adding a period of 24hr normoxia after initial hypoxia (24hr SH + 24hr N) eliminated this increase, demonstrating reversal of TRPM3 enhancement. *, $p < 0.05$, 24h SH vs 24h N; $, $p < 0.05$, 24h SH vs 48h N and 24h SH+ 24h N, Kruskal-Wallis with Dunn's test. (B) *In vitro* 24hr SH did not alter Preg responses compared to in-vitro 24hr Norm. $p > 0.05$, Mann-Whitney test, although it tended to increase the number (or distribution) of cells that responded to a high degree ($p = 0.07$, Kolgorov-Smirnov test) (C) 10d Norm and 10d CIH had equal responses to Preg; n= 36, Norm; n= 19, CIH; #, $p < 0.05$ vs Bsl, $p > 0.05$ Norm vs CIH, Mann-Whitney test.

Author Manuscript Author Manuscript Author Manuscript Author Manuscript

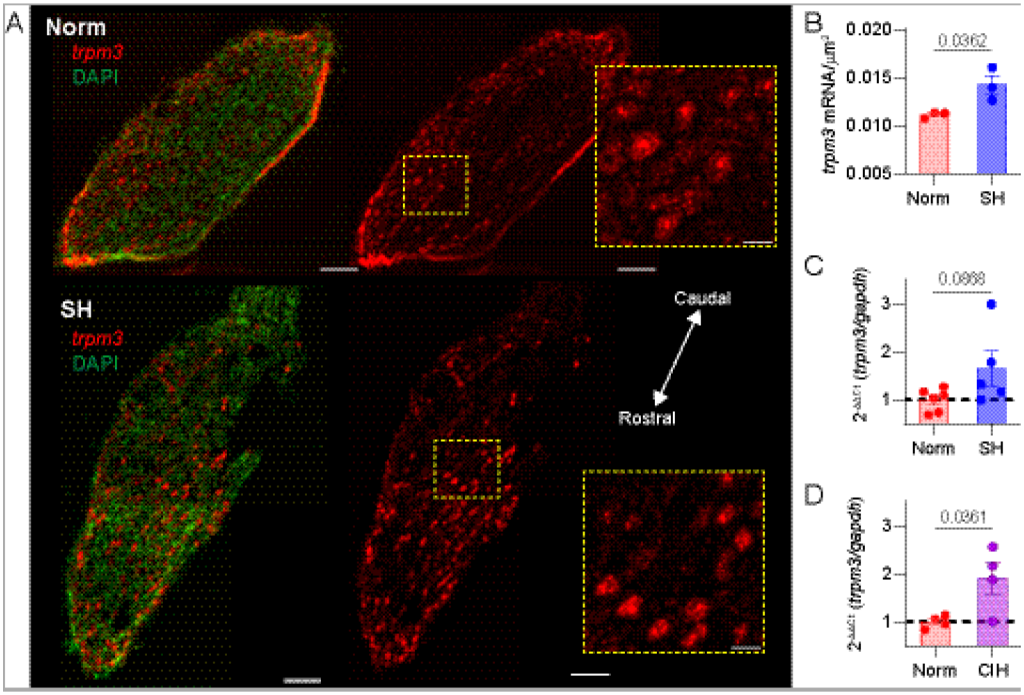

Figure 4. Hypoxia elevates TRPM3 mRNA.

(A). RNAScope demonstrating *trpm3* mRNA expression (red) in the rat nodose ganglion (max projection), and the elevation of signal after SH. Also shown is overlay with DAPI. Scale, 100 μm. Inset shows elevation of *trpm3* after SH. Scale, 25 μm. (B). Quantification of RNAScope *trpm3* mRNA signal in Norm and SH ganglia (n=3 ea). Signal was normalized to tissue size and each "n" represents the average of 2–3 individual sections. (C, D). RT-PCR of *trpm3* normalized to that of *gadph* after SH (C, n=5,6) or CIH (D, n=4 ea). unpaired t-test.